Engineering Structures 198 (2019) 109471

Contents lists available at ScienceDirect

Engineering Structures

journal homepage: www.elsevier.com/locate/engstruct

Numerical study using FE simulation on rectangular RC beams with vertical circular web openings in the shear zones

Ahmed M. Sayed*

Department of Civil Engineering, Engineering Faculty, Assiut University, Assiut, Egypt
Department of Civil and Environmental Engineering, College of Engineering, Majmaah University, Al-Majmaah 11952, Saudi Arabia

ARTICLE INFO

Keywords:
RC beams
Finite element
Vertical opening
Shear load
Opening diameter

ABSTRACT

Transverse and vertical openings are usually created in beams made of reinforced concrete (RC) to accommodate the pipes and ducts used in utilities. The decrease in shear strength because of the openings causes problems in current RC beams. This study investigates the impact of various vertical circular web openings alongside the shear-area span of an RC beam on its shear performance. To this end, a model with three finite element (FE) dimensions was developed, primarily for investigating and analyzing the outcome of this case. Using the ANSYS-V15 FE program, 41 beams were analyzed. The findings of the eight investigational beams were compared with results from previously published works. The devised model was tested to ensure its accurate functioning, using outcomes already attained through experiments. The outcomes of the experimental test proved that the newly devised FE model could be used to calculate the RC beams' shear-load capacity and to accurately predict failure modes. The outcomes revealed that the effect of the vertical-opening diameter on the width of the beam section was greater than the effect of the length of the shear span. Therefore, we concluded that the influence of the opening diameter was greater than the effect of the number of openings.

1. Introduction

Passageways for the pipes for water-supply systems, sewage, electricity, telephone cables, and internet cables are frequently introduced by means of horizontal and vertical openings in the flooring beams. This allows the engineering crew to utilize a building design that uses the dead space above the beam soffit comparatively more efficiently (see Fig. 1).

In several instances, it has been observed that providing horizontal or vertical openings in reinforced concrete (RC) beams results in unwarranted pressures, which may be harmful if a proper assessment and design is not made. Experimental and numerical procedures have revealed that transverse and vertical cracks recurrently appear at the corners of horizontal or vertical openings. These cracks may extremely diminish the RC beams' ultimate load capacity [1–4].

Many examinations [3–8] have been conducted on RC beams with different cross sections (T or rectangular) and web openings to predict the deflection of the load and the cracks, in addition to the eventual conduct of the RC beams. The chief variables under investigation include the horizontal location, dimensions, and number of openings in the beams. A previous study [3–8] revealed that the existence of web openings reduces cracks, as well as decreasing the eventual strength and stiffening, and raises the deflections and cracking breadths of the RC beams. In addition, the beam failures that were tested with openings had primarily been shearing failures, associated with cracks originating around the web openings.

Because existing experimental and numerical research, e.g., [3–8], ignores the impact of the vertical openings on the shear-load capacity, it is challenging to exactly predict the shear-load capacity of RC beams with vertical openings. These vertical openings have a direct effect on the shear resistance of the RC beams because of the decrease in the concrete width, as well as the inability to connect the stirrups in the opening area.

This study focuses on numerically analyzing the impact of vertical circular openings in a rectangular web section in the shear span to see how the RC beams behave. The scope of the study involves the location, number of openings, and dimensions of the vertical openings. Forty-one RC beams were arranged and tested beneath where the point loads were applied in previous studies. Three different vertical circular-opening sizes and locations, together with two dissimilar numbers of openings, were investigated.

The numerical analysis was conducted using ANSYS FE software [9]. In addition, a database of experimental outcomes on RC beams described in the literature [4,10–13] was gathered for use in verifying

* Address: Department of Civil Engineering, Engineering Faculty, Assiut University, Assiut, Egypt.
E-mail address: a.sayed@mu.edu.sa.

https://doi.org/10.1016/j.engstruct.2019.109471
Received 11 April 2019; Received in revised form 20 June 2019; Accepted 31 July 2019

Fig. 1. RC floor beams with vertical pipe openings in the shear zone.

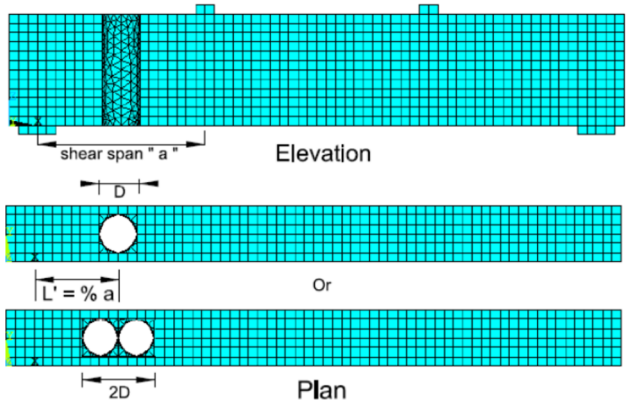

Fig. 2. Numerical FE modeled RC beams with geometrical meshing, and details of the vertical circular openings.

the accuracy of the numerical results obtained through the ANSYS program [9]. The authenticated statistical examination was then used for beneficial parametric studies, wherein the effect of several parameters, together with the location, number of openings, and dimensions of the vertical openings, was examined.

Many other studies, e.g., [14–19], used FE modeling to demonstrate that the behavior of RC members can be simulated accurately, particularly the shear behavior of simply supported RC beams. Consequently, a special FE model was devised that could simulate RC beams with vertical openings and investigate each parameter under static loads.

2. ANSYS finite-element model study

The investigated beams were modeled using the ANSYS-15 general-purpose FE software [9]. The FE numerical analysis was carried out on forty-one RC beams with full dimensions. While analyzing, suitable material models were used to represent the performance of the concrete, steel reinforcement, and plates. These are elaborated in the ANSYS [9] manual set, in addition to the model of the bond-performance interface element.

2.1. Concrete model and properties

A solid element, SOLID65, was applied to model the concrete in ANSYS [9]. The solid element bears eight nodes with three provisional degrees of freedom (DoF) at each node. Moreover, the element can simulate plastic distortion, crushes, and cracks in three orthogonal dimensions. To simulate how concrete actually behaves, ANSYS needs linear isotropic and multi-linear isotropic material attributes to be entered, along with certain supplemental concrete-material attributes [14–18].

The mesh was brought into a square to obtain favorable findings with the tested beam, which was 25 × 25 × 25 mm, as illustrated in Fig. 2. The “merge items” command merges secluded objects that are in the same location. Thereafter, these items are amalgamated into a single unit. Cautionary measures are needed when entities are integrated into a model that has previously been meshed, as the sequence in which the merger takes place is very important.

2.2. Steel reinforcement and plates: Model and properties

To obtain the intrinsic stresses and strains in the reinforcing bars and keep them in their accurate locations, the LINK180 3-D spar element [9] is adhered to. This component can be applied to modeling trusses, sagging cables, links, springs, etc. The component is a uniaxial tension-compression element with three DoF at every single node: transformations in the nodal x-, y-, and z-directions. Flexibility, rotation, creep, large strain, and large deflection abilities are involved. The elements are defined by two nodes, the cross-sectional zone input via the section type and section data commands, and the material properties.

The steel plates located at the supports and used for applied loads of RC beams are modeled using SOLID186 elements [9]. This element bears 20 nodes with three DoF for each single node transformation in the x-, y-, and z-directions. SOLID186 is an advanced-order 3D 20-node solid element that displays quadratic displacement behavior. The element supports creep, plasticity, hyperelasticity, large deflection, stress stiffening, and large strain capabilities.

The steel reinforcement and plates unified into the FE models were intended to be linearly flexible constituents with a Poisson’s ratio of 0.3 and an elastic modulus of 210 GPa [17,18]. The yield stress differs depending on where the element is used.

Table 1
Summary of RC beams calculated through FE modeling in the current study.

FE model based on	Beam specimen	Beam dimensions $b \times t \times L$ (mm)	Concrete f_{cu} (MPa)	Steel reinforcement		Vertical opening parameters		
				Longitudinal f_y (MPa)	Stirrups f_y (MPa)	Number	Diameter D (mm)	Location % a
Shoeib and Sedawy [4]	B1-0-0-0	150 × 300 × 1650	31.0	360	240	–	–	–
	B2-ϕ7.5-(A)-0	150 × 300 × 1650	31.0	360	240	1-H	75	50%a
	B3-ϕ15-(A)-0	150 × 300 × 1650	31.0	360	240	1-H	150	50%a
Gonzalez-Libreros et al. [10]	S1-CONTROL	150 × 300 × 3000	23.3	545	527	–	–	–
	S2-CONTROL	150 × 300 × 3000	24.7	545	527	–	–	–
Azam et al. [11]	S150-N	250 × 400 × 2700	61.0	494	365	–	–	–
Khalifa [12]	B-C	150 × 260 × 2700	35.0	400	350	–	–	–
Dias et al. [13]	REF	150 × 300 × 2600	50.2	566.7	564.1	–	–	–
New FE model	S1-G-1O-D50-0.25a	150 × 300 × 3000	23.3	545	527	1	50	25% a
	S1-G-1O-D50-0.50a	150 × 300 × 3000	23.3	545	527	1	50	50% a
	S1-G-1O-D50-0.75a	150 × 300 × 3000	23.3	545	527	1	50	75% a
	S1-G-1O-D100-0.25a	150 × 300 × 3000	23.3	545	527	1	100	25% a
	S1-G-1O-D100-0.50a	150 × 300 × 3000	23.3	545	527	1	100	50% a
	S1-G-1O-D100-0.75a	150 × 300 × 3000	23.3	545	527	1	100	75% a
	S1-G-2O-D100-0.25a	150 × 300 × 3000	23.3	545	527	2	100	25% a
	S1-G-2O-D100-0.50a	150 × 300 × 3000	23.3	545	527	2	100	50% a
	S1-G-2O-D100-0.75a	150 × 300 × 3000	23.3	545	527	2	100	75% a
	S2-G-1O-D50-0.25a	150 × 300 × 3000	24.7	545	527	1	50	25% a
	S2-G-1O-D50-0.50a	150 × 300 × 3000	24.7	545	527	1	50	50% a
	S2-G-1O-D50-0.75a	150 × 300 × 3000	24.7	545	527	1	50	75% a
	S2-G-1O-D100-0.25a	150 × 300 × 3000	24.7	545	527	1	100	25% a
	S2-G-1O-D100-0.50a	150 × 300 × 3000	24.7	545	527	1	100	50% a
	S2-G-1O-D100-0.75a	150 × 300 × 3000	24.7	545	527	1	100	75% a
	S2-G-2O-D100-0.25a	150 × 300 × 3000	24.7	545	527	2	100	25% a
	S2-G-2O-D100-0.50a	150 × 300 × 3000	24.7	545	527	2	100	50% a
	S2-G-2O-D100-0.75a	150 × 300 × 3000	24.7	545	527	2	100	75% a
	A-1O-D50-0.25a	250 × 400 × 2700	61.0	494	365	1	50	25% a
	A-1O-D50-0.50a	250 × 400 × 2700	61.0	494	365	1	50	50% a
	A-1O-D50-0.75a	250 × 400 × 2700	61.0	494	365	1	50	75% a
	A-1O-D100-0.25a	250 × 400 × 2700	61.0	494	365	1	100	25% a
	A-1O-D100-0.50a	250 × 400 × 2700	61.0	494	365	1	100	50% a
	A-1O-D100-0.75a	250 × 400 × 2700	61.0	494	365	1	100	75% a
	A-1O-D150-0.25a	250 × 400 × 2700	61.0	494	365	1	150	25% a
	A-1O-D150-0.50a	250 × 400 × 2700	61.0	494	365	1	150	50% a
	A-1O-D150-0.75a	250 × 400 × 2700	61.0	494	365	1	150	75% a
	A-2O-D100-0.25a	250 × 400 × 2700	61.0	494	365	2	100	25% a
	A-2O-D100-0.50a	250 × 400 × 2700	61.0	494	365	2	100	50% a
	A-2O-D100-0.75a	250 × 400 × 2700	61.0	494	365	2	100	75% a
	S-1O-D100-0.25a	150 × 300 × 1650	31.0	360	240	1	100	25% a
	S-1O-D100-0.50a	150 × 300 × 1650	31.0	360	240	1	100	50% a
	S-1O-D100-0.75a	150 × 300 × 1650	31.0	360	240	1	100	75% a

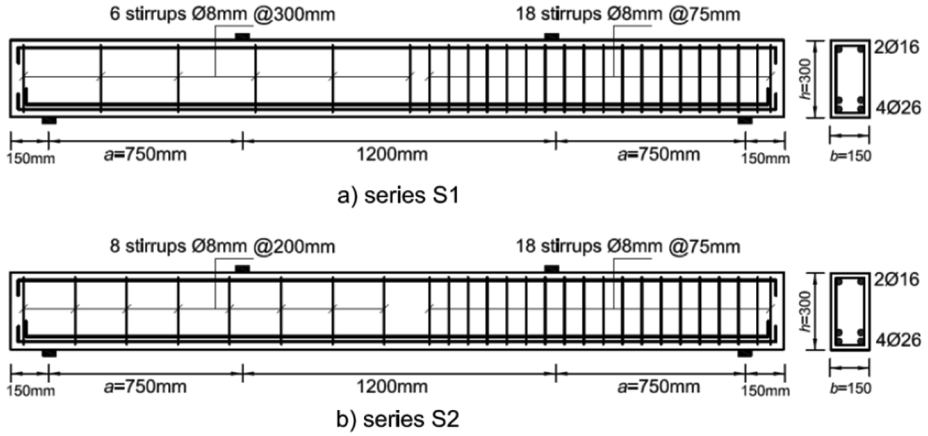

Fig. 3. RC beams illustrated geometrically in accordance with an already published treatise by Gonzalez-Libreros et al. [10].

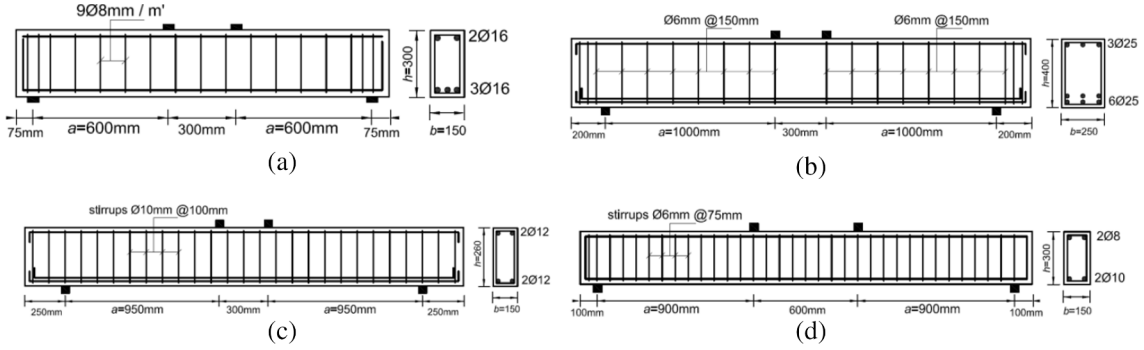

Fig. 4. RC beams illustrated geometrically in accordance with an already published treatise by (a) Shoeib and Sedawy [4], (b) Azam et al. [11], (c) Khalifa [12], and (d) Dias et al. [13].

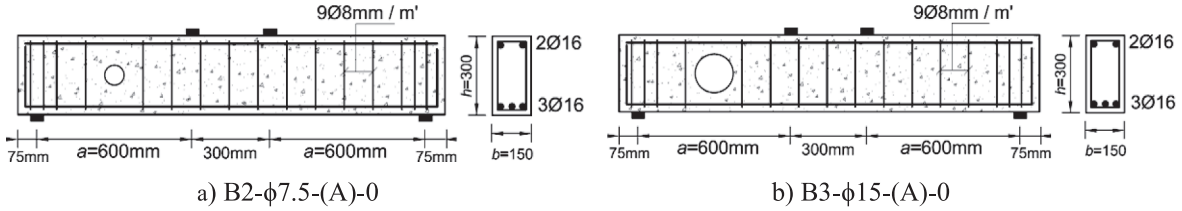

Fig. 5. RC beams with horizontal circular openings illustrated geometrically in accordance with an already published treatise by Shoeib and Sedawy [4].

Table 2
Comparing ultimate failure loads and maximum deflection for investigational and FE outcomes.

FE model based on	Beam specimen	Ultimate load			Maximum deflection at ultimate load		
		Experimental (kN)	FE (kN)	P_{Exp}/P_{FE}	Experimental (mm)	FE (mm)	Δ_{Exp}/Δ_{FE}
Shoeib and Sedawy [4]	B1-0-0-0	277.5	274.89	1.009	10.13	10.00	1.013
	B2-ϕ7.5-(A)-0	180.5	182.75	0.988	9.603	10.55	0.910
	B3-ϕ15-(A)-0	96.0	94.15	1.020	5.81	5.91	0.983
Gonzalez-Libreros et al. [10]	S1-CONTROL	230.5	227.43	1.013	15.40	15.08	1.021
	S2-CONTROL	259.3	255.36	1.015	14.50	15.30	0.948
Azam et al. [11]	S150-N	613.9	600.60	1.022	12.70	12.20	1.041
Khalifa [12]	B-C	47.03	48.06	0.979	11.67	13.80	0.846
Dias et al. [13]	REF	62.3	63.35	0.983	8.30	9.20	0.902

3. Numerical model studies

Numerical FE simulations were carried out on forty-one RC beams, with variable geometrical cross sections and lengths considered in the present research. Eight of these beams are control beams; six of them have no openings and two have horizontal circular openings, according to previously published work [4,10–13]. Twenty-four beams have a vertical opening with 50, 100, and 150-mm diameters created 0.25, 0.5, and 0.75 shear spans from the centerline of the vertical opening to the centerline of support. The last nine beams have two circular openings

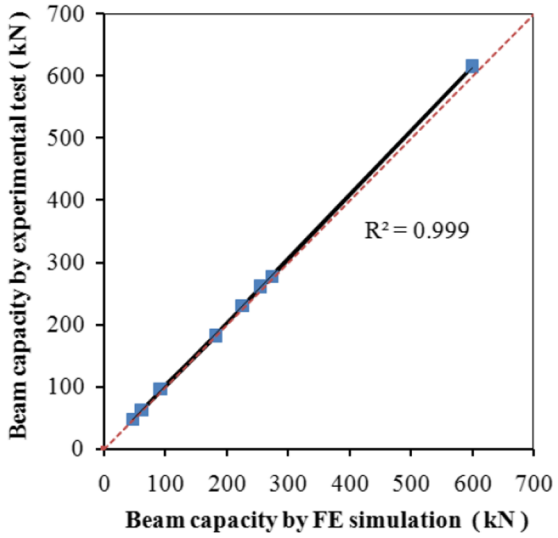

Fig. 6. Comparing the experimental and modeled values for the ultimate-failure load capacity.

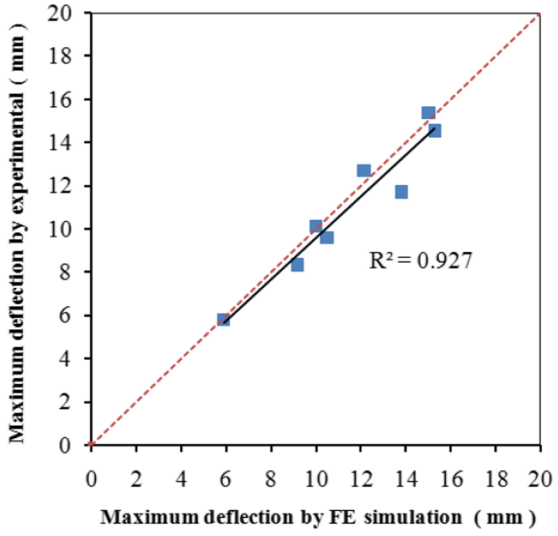

Fig. 7. Comparing the experimental and modeled values for the maximum deflection at the ultimate load.

with 100-mm diameters created at 0.25, 0.5, and 0.75 shear spans. The RC beams from previously published work [4,10–13] and beams with vertical circular openings are shown in Table 1. The RC beams with applied loads, reinforcement, and dimensions, as illustrated in Figs. 3–5, were tested to ratify the accuracy of the FE model.

4. Comparing the FE analysis with the experimental results

To analyze how reliable and valid the FE simulation is, a broad verification was conducted by means of a series of investigational data that exists in the literature [4,10–13]. The database under consideration contains the findings of eight empirical tests, including the consequences of experiments with six RC beams' failure in the shear zone (shear failure) [4,10,11], and two RC beams' failure in the maximum moment zone (flexural failure) [12,13].

Table 2 shows the ultimate failure loads for both experimental and analytical results with the ratios between them. The experimental and analytical values are compared graphically in Figs. 6 and 7. In this table and figures, for the ultimate load capacities, the mean value of P_{Exp}/P_{FE} is 1.004, the coefficient of correlation is 0.999, and the compatible coefficient of variation is 1.757%. For the maximum deflection at the ultimate load, the mean value of Δ_{Exp}/Δ_{FE} is 0.958, the coefficient of correlation is 0.927, and the compatible coefficient of variation is 6.83%. These values illustrate that, from a statistical perspective, the FE simulation is an exceptional match and can be adopted for all RC beams with both shear and flexural failures that were considered in the analysis.

Fig. 8 presents the load-displacement curves for the samples employed in the experiments and the consequential FE analysis. When one compares the load deflections derived from the experiments' conclusions with the ones obtained from the FE simulation of RC beams devoid of openings, one can observe an exceptional match between them.

The behavior of the FE models involving all the samples, including deformed shapes, failure loads, and failure modes, was noted. Figs. 9–11 demonstrate the deformations, failure modes, and positions for the investigational samples and the conforming FE simulation. While comparing the deformations and failure modes with positions obtained from the investigational results with the ones attained from the FE simulation for RC beams in both shear—with and without openings—and flexural failure modes, an excellent match can be observed.

5. Numerical results and discussion

The outcomes shown in the following segments are expressed relating to the eventual shear-load holding capacities, load–deflection relationships, and failure modes.

5.1. Crack patterns, shear capacity, and failure modes

The crack patterns, shear capacity, and failure modes were observed for all beams for the different beam series, as follows. For all the tested beams with a vertical opening, the first crack was observed at the bottom concrete surface around the opening. This crack occurred at a cracking-load level less than the control beam. By increasing the applied load, the crack increases more in a shear zone that has a vertical opening in the web than the other sides that are not open, as shown in Fig. 12. The final failure mode was a shear-failure type through the vertical opening. The test specimen failed at a corresponding applied ultimate shear load-carrying capacity less than the control beam. These results were measured for all beams with a vertical opening for different opening diameters, as shown in Fig. 12. The increase in the opening diameter increases the crack in the shear zone with a vertical opening and decreases the crack in the other sides that are not open.

5.2. Load–deflection relationships

The relationships between the applied load and the beam mid-span deflection of the tested specimens are presented in Figs. 13 and 14. Generally, the deflection at any level for a beam with a vertical opening is greater than that of a control beam with the same load. However, the maximum measured values of the ultimate loads and deflections at a failure level for beams that have a vertical opening are smaller than those for the control beams.

As demonstrated in Fig. 13, the load-deflection curves of the beams that have a 100-mm diameter vertical opening at the different locations (0.25, 0.50, and 0.75) of the shear span do not differ significantly.

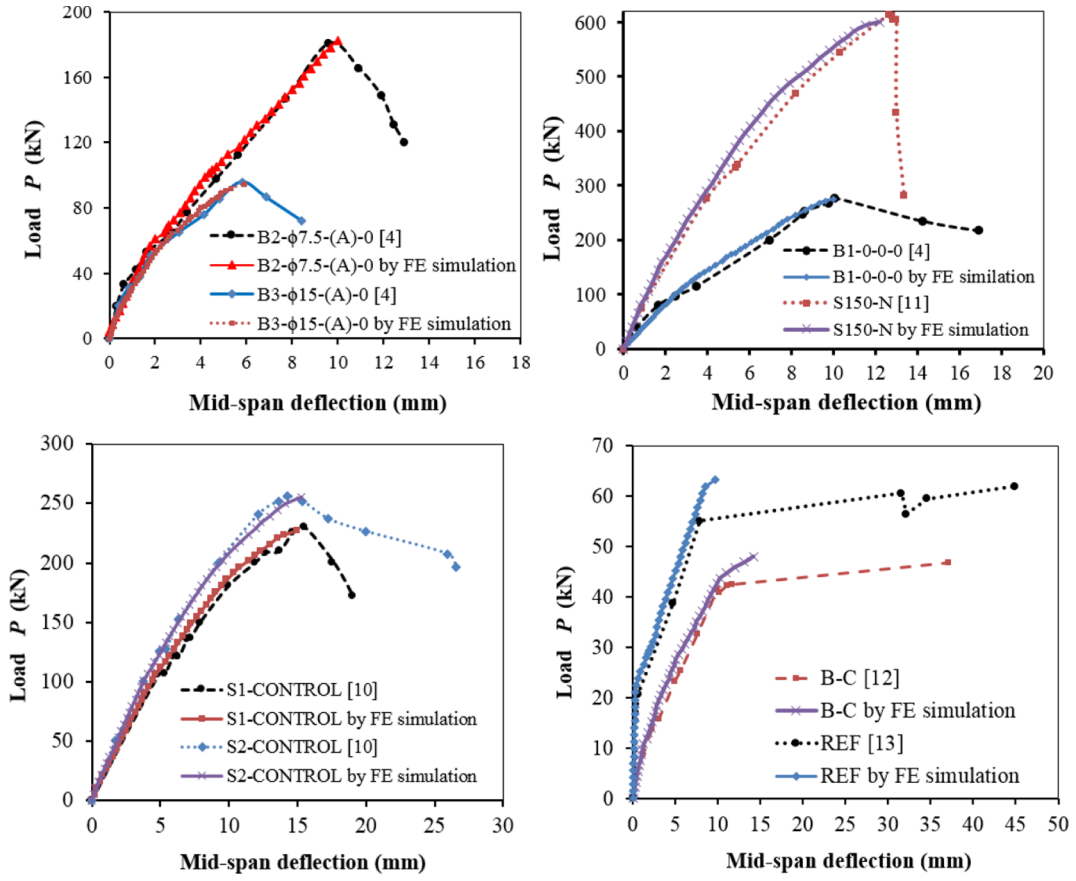

Fig. 8. Load-deflection curves acquired from experimental results, Shoeib & Sedawy [4], Gonzalez-Libreros et al. [10], Azam et al. [11], Khalifa [12], Dias et al. [13], and FE simulation.

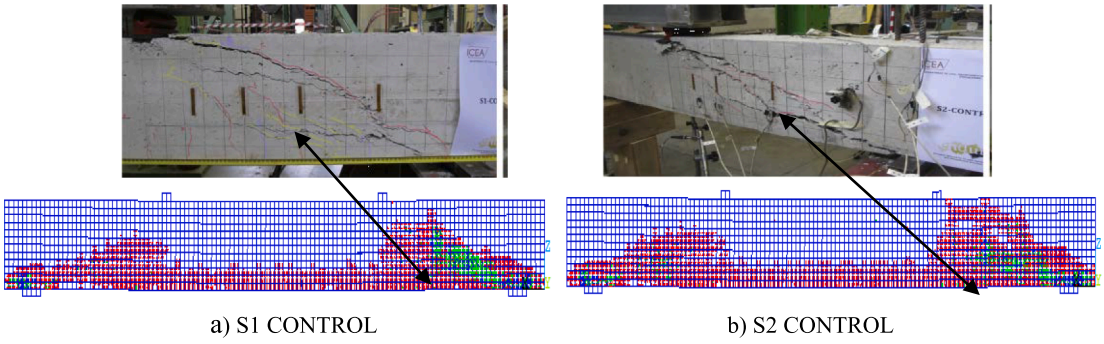

Fig. 9. Deformations and failure modes with locations gained from (a) experiments (Gonzalez-Libreros et al. [10]) and (b) FE simulations.

Therefore, the average load-deflection for each vertical opening for the three different locations was taken as a single curve, as shown in Fig. 14. It can be observed from the figure that increasing the diameter of the vertical opening decreases the maximum deflection at the failure load, and the ultimate load capacity decreases. This is ascribable to the decreasing stiffness of the RC beams by increasing the diameter of the vertical opening in the shear span. The rate and value of the decrease differs from the control beam to the other tested beams, as can be seen in Table 3.

5.3. *Influence of the vertical-opening diameter*

The vertical-opening diameter is a significant feature that directly influences the strength and stiffness of the RC beam. The vertical-

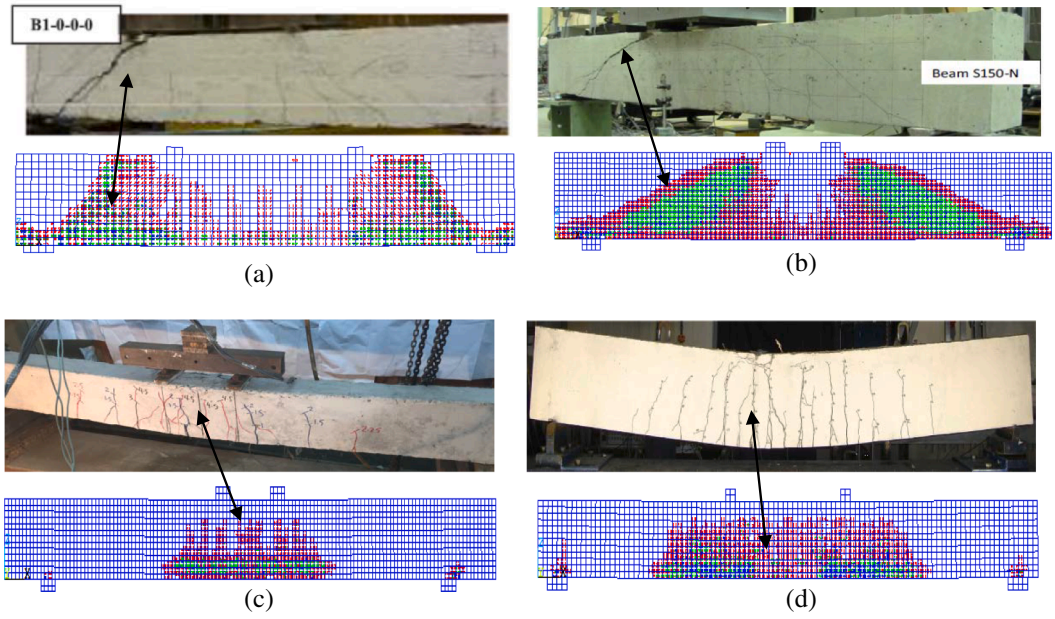

Fig. 10. Deformations and failure modes with locations gained from experiments, (a) Shoeib & Sedawy [4], (b) Azam et al. [11], (c) Khalifa [12], (d) Dias et al. [13], and FE simulations.

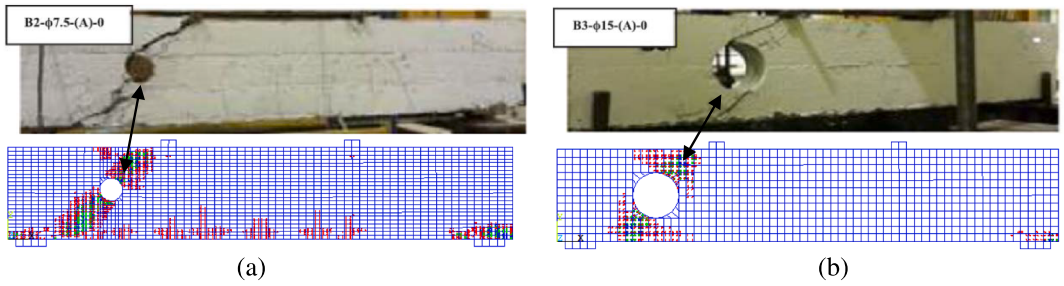

Fig. 11. Deformations and failure modes with locations gained from experiments, Shoeib & Sedawy [4], and FE simulations for beams (a) B2-ϕ7.5-(A)-0 and (b) B3-ϕ15-(A)-0.

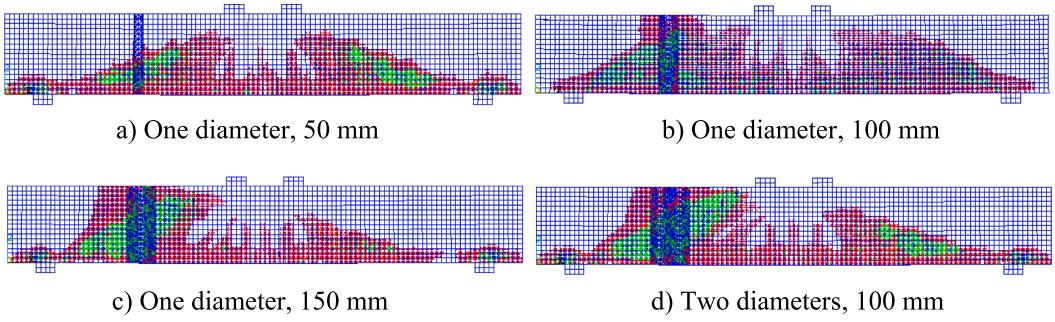

Fig. 12. Crack pattern and failure mode of RC beams with a vertical opening created at 0.5 of the shear span.

opening diameter substantially affects the mid-span deflection, together with the final shear-load capacity of the beams, as shown in Fig. 15. When the vertical-opening diameter increases, the eventual shear-load capacity decreases. The location of the opening in the shear span for the same diameter has no significant effect; the difference was found to be less than 2% for all the diameters. The main factor that controls the shear capacity is the diameter of the vertical opening. It can be concluded that the effect of the opening diameter is greater than the effect

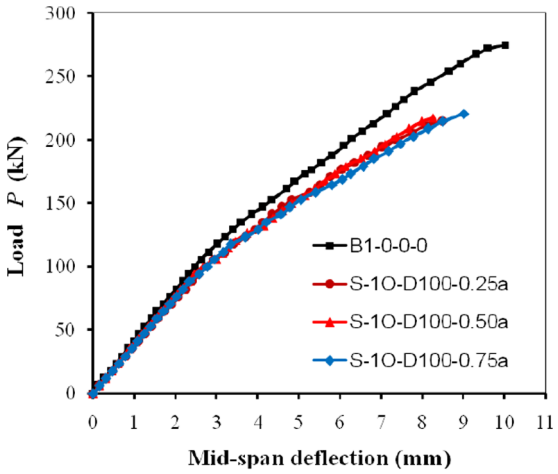

Fig. 13. Load-deflection curves obtained from FE simulation for RC beams that have one vertical opening (100 mm) with different locations in the shear zone.

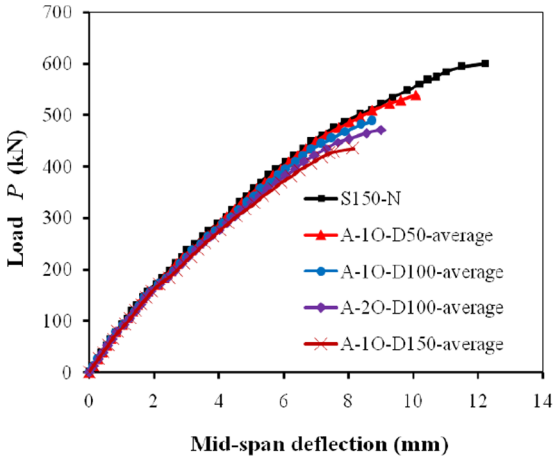

Fig. 14. Average of load-deflection curves obtained from FE simulation for RC beams that have different vertical-opening diameters.

of the number of openings, as shown in Fig. 15.

Fig. 16 shows that the impact of the vertical opening diameter on the width of the beam section is greater than the effect on the length of the shear span. This is illustrated by the slope of the straight line between the results of the FE tested beams. From the above discussion, it can be concluded that the influence of the opening diameter is greater than the effect of the number of openings. This is ascribable to the decrease in the RC beams' stiffness by decreasing the actual width of the beam cross sections by increasing the diameter of the vertical opening in the shear zone.

As can be seen in Fig. 16, the coefficient of correlation (R^2) is 0.847 for the influence of the opening diameter on the beam width and 0.940 for the shear span. These values were obtained by using a linear-regression line to determine the influence of the vertical-opening diameter on both the beam width and the shear span. From a statistical perspective, these values show that the effect of the opening diameter along the shear span is more uniform than the width of the concrete-beam section.

6. Conclusions

In this study, finite element (FE) modeling was introduced as a tool to predict the RC beams' shear-load capacity with a vertical opening. Parametric studies were carried out to evaluate the impacts of the location, number of openings, and dimensions of the vertical openings on the capacity of the ultimate shear load, and the failure modes of the RC beams. The results of the FE model were compared with literature dealing with similar structures relating to test geometries. The tests results showed that the FE model could be a more precise tool for predicting the failure mode, as well as assessing the ultimate load capacity.

The mean value of P_{Exp}/P_{FE} was found to be 1.004 for beams without a vertical opening; the coefficient of correlation was 0.999 and the analogous coefficient of variation was 1.757%. An evaluation of the FE models showed that increasing the vertical circular-opening diameter decreased the maximum deflection at the failure load and the ultimate load capacity. In addition, the influence of the opening diameter was greater than the effect of the number of openings on the latter parameters. Finally, it was proved that the vertical-opening diameter that was set on the width of the beam section had a greater effect than the length of the shear span on the maximum deflection at the failure load and the ultimate load capacity.

Acknowledgments

The researcher especially thanks the Deanship of Scientific Research at Majmaah University for its continuous support of this work under Project No. 1439-46.

Table 3
Summary of the RC beams' FE test results from the present study.

FE model based on	Beam specimen	FE ultimate load (kN)	Decrease in ultimate load (kN)	% Decrease $P_{dec.}/P_{u.control}$
Shoeib and Sedawy [4]	B1-0-0-0	274.89	–	–
Gonzalez-Libreros et al. [10]	S1-CONTROL	227.43	–	–
	S2-CONTROL	255.36	–	–
Azam et al. [11]	S150-N	600.60	–	–
Khalifa [12]	B-C	48.06	–	–
Dias et al. [13]	REF	63.35	–	–
New FE model	S1-G-1O-D50-0.25a	203.49	23.94	10.53
	S1-G-1O-D50-0.50a	199.50	27.93	12.28
	S1-G-1O-D50-0.75a	204.82	22.61	9.94
	S1-G-1O-D100-0.25a	175.56	51.87	22.81
	S1-G-1O-D100-0.50a	172.90	54.53	23.98
	S1-G-1O-D100-0.75a	178.22	49.21	21.64
	S1-G-2O-D100-0.25a	143.64	83.79	36.84
	S1-G-2O-D100-0.50a	140.98	86.45	38.01
	S1-G-2O-D100-0.75a	143.64	83.79	36.84
	S2-G-1O-D50-0.25a	228.76	26.60	10.42
	S2-G-1O-D50-0.50a	223.44	31.92	12.50
	S2-G-1O-D50-0.75a	228.76	26.60	10.42
	S2-G-1O-D100-0.25a	199.50	55.86	21.88
	S2-G-1O-D100-0.50a	202.16	53.20	20.83
	S2-G-1O-D100-0.75a	207.48	47.88	18.75
	S2-G-2O-D100-0.25a	167.58	87.78	34.38
	S2-G-2O-D100-0.50a	167.58	87.78	34.38
	S2-G-2O-D100-0.75a	170.24	85.12	33.33
	A-1O-D50-0.25a	537.90	62.70	10.44
	A-1O-D50-0.50a	528.00	72.60	12.09
	A-1O-D50-0.75a	541.20	59.40	9.89
	A-1O-D100-0.25a	488.40	112.20	18.68
	A-1O-D100-0.50a	481.80	118.80	19.78
	A-1O-D100-0.75a	498.30	102.30	17.03
	A-1O-D150-0.25a	429.00	171.60	28.57
	A-1O-D150-0.50a	421.99	178.61	29.74
	A-1O-D150-0.75a	435.60	165.00	27.47
	A-2O-D100-0.25a	448.80	151.80	25.27
	A-2O-D100-0.50a	455.40	145.20	24.18
	A-2O-D100-0.75a	471.90	128.70	21.43
	S-1O-D100-0.25a	214.62	60.27	21.93
	S-1O-D100-0.50a	217.56	57.33	20.86
	S-1O-D100-0.75a	220.50	54.39	19.79

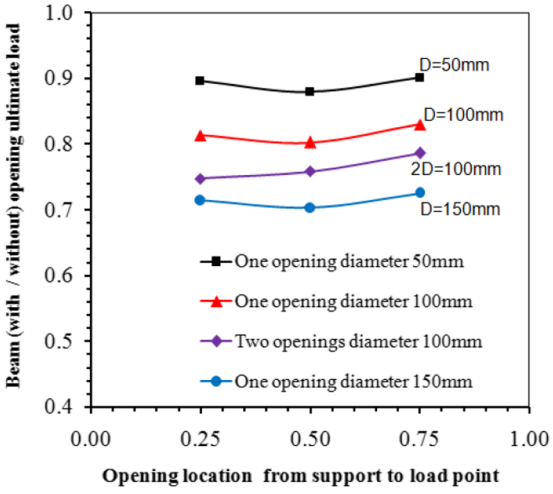

Fig. 15. Relation between the ratio of the ultimate load of the beams with openings and that of the control beams and the influence of the vertical-opening locations.

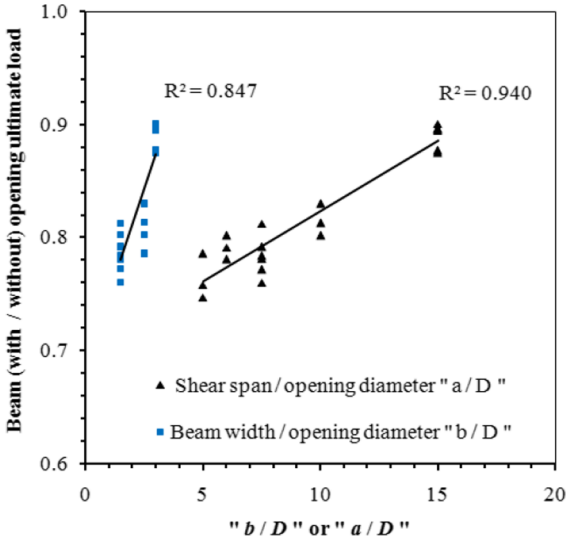

Fig. 16. Relation between the ratio of the ultimate load of the beams with openings and the control beam, and the influence of the beam width and shear span on the vertical-opening diameter.

Appendix A. Supplementary material

Supplementary data to this article can be found online at https://doi.org/10.1016/j.engstruct.2019.109471.

References

[1] Abou El-Mal HSS, Sherbini AS, Sallam HEM. Locating the site of diagonal tension crack initiation and path in reinforced concrete beams. Ain Shams Eng J 2015;6:17–24.

[2] Abou El-Mal HSS, Sherbini AS, Sallam HEM. Structural behavior of RC beams containing a pre- diagonal tension crack. Latin Am J Solids Struct 2018;15(7). e82, 16 pp.

[3] Abdul-Razzaq KS, Abdul-Kareem MM. Innovative use of steel plates to strengthen flange openings in reinforced concrete T-beams. Structures 2018;16:269–87.

[4] Shoeib AE, Sedawy AE. Shear strength reduction due to introduced opening in loaded RC beams. J Build Eng 2017;13:28–40.

[5] Herrera L, Anacleto-Lupianez S, Lemnitzer A. Experimental performance of RC moment frame beams with rectangular openings. Eng Struct 2017;152:149–67.

[6] Nie XF, Zhang SS, Teng JG, Chen GM. Experimental study on RC T-section beams with an FRP-strengthened web opening. Compos Struct 2018;185:273–85.

[7] Elsanadedy HM, Al-Salloum YA, Almusallam TH, Alshenawy AO, Abbas H. Experimental and numerical study on FRP-upgraded RC beams with large rectangular web openings in shear zones. Constr Build Mater 2019;194:322–43.

[8] Aykac B, Kalkan I, Aykac S, Egriboz YE. Flexural behavior of RC beams with regular square or circular web openings. Eng Struct 2013;56:2165–74.

[9] ANSYS User's Manual, Version (15) Swanson Analysis Systems, Inc, 2015.

[10] Gonzalez-Libreros JH, Sneed LH, D'Antino T, Pellegrino C. Behavior of RC beams strengthened in shear with FRP and FRCM composites. Eng Struct 2017;150:830–42.

[11] Azam R, Soudki K, West JS, Noël M. Strengthening of shear-critical RC beams: Alternatives to externally bonded CFRP sheets. Constr Build Mater 2017;151:494–503.

[12] Khalifa AM. Flexural performance of RC beams strengthened with near surface mounted CFRP strips. Alexandria Eng J 2016;55:1497–505.

[13] Dias SJE, Barros JAO, Janwaen W. Behavior of RC beams flexurally strengthened with NSM CFRP laminates. Compos Struct 2018;201:363–76.

[14] Terec L, Bugnariu T, Păstrav M. Non –linear analysis of reinforced concrete frames strengthened with in filled walls. Romanian J Mater 2010;40(3):214–21.

[15] Kwan AKH, Dai H, Cheung YK. Non-Linear seismic response of reinforced concrete slit shear walls. J Sound Vibr 1999;226(4):701–18.

[16] Sayed AM, Xin W, Zhishen W. Finite element modeling of the shear capacity of RC beams strengthened with FRP sheets by considering different failure modes. Constr Build Mater 2014;59:169–79.

[17] Sayed AM, Diab HM. Modeling of the axial load capacity of RC columns strengthened with steel jacketing under preloading based on FE simulation. Model Simulat Eng 2019;2019(8653247):8.

[18] D. Kachlakev, T. Miller, S. Yim, Finite element modeling of reinforced concrete structures strengthened with FRP laminates, Oregon Dept. of Transportation, USA, Res. Group, Final Rep. SPR 316, 2001.

[19] Hassan NZ, Sherif AG, Zamarawy AH. Finite element analysis of reinforced concrete beams with opening strengthened using FRP. Ain Shams Eng J 2017;8:531–7.